Numerical evaluation of 3D geoelectrical resistivity imaging for environmental and engineering investigations using orthogonal 2D profiles

A. P. Aizebeokhai[1*], A. I. Olayinka[2], and V. S. Singh[3]; [1]Department of Physics, Covenant University; [2]Department of Geology, University of Ibadan; [3]National Geophysical Research Institute

Summary

Field design for 3D data acquisition in geoelectrical resistivity imaging using a net of orthogonal sets of 2D profiles was numerically investigated. A series of 2D apparent resistivity pseudosections were generated over a synthetic horst structure representing the geological environment of a crystalline basement in low latitude areas using RES2DMOD code. Different minimum electrode separations and inter-line spacing were used with a view of determining the optimum inter-line spacing relative to the minimum electrode separation. The 2D apparent resistivity data were collated to 3D data set and then inverted using RES3DINV, a full 3D inversion code. The relative effectiveness and imaging capabilities of Wenner-alpha (WA), Wenner-beta (WB), Wenner-Schlumberger (WSC), dipole-dipole (DDP), pole-dipole (PDP), and pole-pole (PP) arrays to image the structure using a net of orthogonal set of 2D profiles are presented. The normalized average sensitivity of the inversion results show that WSC, DDP, and PDP arrays are more sensitive to the 3D structure investigated. Inter-line spacing of not greater than four times the minimum electrode separation gives reasonable resolution.

Introduction

Geoelectrical resistivity imaging has played an important role in addressing a wide variety of hydrological, environmental and geotechnical issues. The goal of geoelectrical resistivity surveys is to determine the distribution of subsurface resistivity by taking measurements of the potential difference. For a typical inhomogeneous subsurface, the true resistivity is estimated by carrying out inversion on the observed apparent resistivity values. The classical approach for resistivity surveys assumes a homogeneous subsurface and smooth potential field; thus it is inadequate in environmental and engineering investigations where the geology is usually complex, subtle and multi-scale such that both lateral and vertical variations can be very rapid. 2D geoelectrical resistivity imaging, in which the resistivity is assumed to vary both laterally and vertically along the survey line but constant in the perpendicular direction, often produce misleading subsurface images due to out-of-plane resistivity anomaly, and the inherent three-dimensional nature of geological structures and petrophysical properties and/or contaminants. Hence, a 3D geoelectrical resistivity imaging should, in theory, give a more accurate and reliable results especially in highly heterogeneous subsurface associated with environmental and engineering investigation sites.

What constitute a 3D data set that would yield significant 3D information is less understood. Ideally, a 3D data set should constitute a survey in which measurements are made in all possible directions. In the 3D geoelectrical resistivity surveying currently in practice, electrodes are commonly arranged in square or rectangular grids with constant electrode spacing in both x- and y-directions. Most practical/large scale 3D geoelectrical resistivity surveys would involve grids of 16×16 (256 electrodes) or much more, which is far more than that available in many multi-electrode resistivity systems. The roll-along technique (Dahlin and Bernstone, 1997) could be used to get around this limitation. But this technique could be tedious and cumbersome, and therefore may not be economical in large scale 3D geoelectrical resistivity imaging. Pole-pole array has been commonly used in 3D surveys because it has the highest number of possible independent measurements and the widest horizontal coverage. The pole-pole array consists of one current and one potential electrode with the second current and potential electrodes at infinite distances. Finding suitable locations for these electrodes at infinity to satisfy the theoretical requirement is often difficult in practical surveys. The contributions of the electrodes at infinity to the observed data can be significant making it difficult for the measured data to satisfy reciprocity condition (Park and Van, 1991). Apart from these limitations, pole-pole array is highly susceptible to telluric noise capable of degrading the quality of the observed data and hence the inversion models. Hence, a more realistic and practical 3D data acquisition geometry that would allow reasonable flexibility in the choice of electrode configuration is needed.

In this paper, the effectiveness of collating orthogonal set of 2D profiles to archive 3D data set which are processed using a full 3D inversion code is numerically evaluated. In order to investigate the relative effectiveness and imaging capabilities of selected arrays: Wenner-alpha (WA), Wenner-beta (WB), Wenner-Schlumberger (WSC), dipole-dipole (DDP), pole-dipole (PDP), and pole-pole (PP), a 3D horst structure model (Figure 1) which simulates a typical weathered or fractured profile in crystalline basement complex in tropical areas was designed. This geological condition is commonly associated with geophysical applications for hydrogeological, environmental and engineering investigations. Hence it is important to investigate the response of this structure to 3D geoelectrical resistivity surveying with a combination of orthogonal sets of 2D resistivity imaging for different electrode configurations. Differences in the arrays spatial resolution, tendency to produce artefacts in 3D images, the deviation from true resistivity model values and maximum depth of investigation as well as the optimum spacing between the orthogonal sets of 2D lines (inter-line spacing) relative to the minimum electrode separation required to form a significant 3D data set that would yield reasonable 3D inversion model are presented.

Methods

Synthetic Apparent Resistivity Pseudosection

The 3D horst structure was approximated into a series of 2D model structures separated with a constant interval in parallel and perpendicular directions. Synthetic apparent resistivity data were calculated over the resulting

orthogonal set of 2D profiles using RES2DMOD forward modelling code for selected arrays. The parallel 2D profiles which run in the west-east direction were denoted as in-lines while those in the perpendicular direction were denoted as cross-lines. Electrode layouts with different minimum separations a and inter-line spacing, L (a = 2 m, 4 m, 5 m and 10 m; $L = a$, $2a$, $2.5a$, $4a$, $5a$ and $10a$) were used. The series of 2D model structures were subdivided into a number of homogeneous and isotropic blocks using a rectangular mesh. The model resistivity value of each block in the mesh was supplied using an input text file. The 2D modelling accounts for 3D effect of current sources; thus the resistivity is allowed to vary arbitrarily along the profile and with depth, but with an infinite perpendicular extension. The finite difference method (Dey and Morrison, 1979), which basically determines the potentials at the nodes of the rectangular mesh, was employed in the calculation of the potential distribution. A double precision, which slightly takes a longer time but significantly more accurate, was used in the calculations of the potential distribution. The apparent resistivity values were normalised with the values of a homogeneous earth model so as to reduce the errors in the calculated potential values. The calculation errors are often less than 5%. The forward modelling grid used consists of four nodes per unit electrode. The calculated apparent resistivity values for each 2D profile were contaminated with 5% Gaussian noise (Press et al., 1996) so as to simulate field conditions.

Data Collation and Inversion

The synthetic apparent resistivity data computed for the series of approximated 2D model structures were then collated to 3D data set using RES2DINV inversion software (Loke and Barker, 1996). The collations arranged the 2D apparent resistivity data and the electrode layouts in rectangular or square grids according the coordinates and direction of each profile used, and electrodes positions in the profile. Thus, the number of electrodes in each 2D profile, number of profiles collated and their directions determine the size and pattern of the electrode grid obtained. The collated 3D data sets were inverted using RES3DINV computer code which automatically determines a 3D model of resistivity distribution using apparent resistivity data obtained from a 3D resistivity imaging survey (Li and Oldenburg, 1994; White et al., 2001). Ideally, the electrodes used for such surveys are arranged in squares or rectangular grids. The inversion routine used by the RES3DINV program is based on the smoothness constrained least-squares method (deGroot-Hedlin and Constable, 1990; Sasaki, 1992) which is based on the following equations:

$$\{J^T J + \mu(f_x f_x^T + f_z f_z^T)\}d = J^T g, \qquad 1$$

where f_x is the horizontal flatness, f_z is the vertical flatness, μ is the damping factor, J is the Jacobian matrix of partial derivatives, d is the model perturbation vector, g is the discrepancy vector, and J^T is the transpose of J.

The program allows users to adjust the damping factor and the flatness filters in equation 1 to suit the data set being inverted. A trial and error method was used in selecting the appropriate initial damping factor for each data set inverted. Initial damping factor of between 0.120 - 0.150 were used. For the same model with the same electrode grid size, a different damping factor may work best for different arrays. After each iterating process, the inversion subroutine generally reduces the damping factor used; a minimum limit (one-tenth of the value of the initial damping factor) was set to stabilize the inversion process. The damping factors were optimised so as to reduce the number of iterations the program requires to converge by finding the optimum damping factor that gives the least RMS error; however, this increases the time taken per iterations.

Results

The 3D inversions images of the synthetic model for the electrode configurations considered were carefully examined. The horizontal depth slices of the 3D inversion images for a grid size of 21x21 and inter-line spacing of $4a$, where a is the minimum electrode separation, obtained using smoothness constrained inversion for the selected arrays are presented in Figures 2 to 7 as representatives. The average sensitivity values for the images presented below are: 0.55 (WA), 0.48 (WB), 1.03 (WSC), 1.47 (DDP), 1.48 (PDP) and 0.54 (PP). Similar sensitivity trends are obtained in the inversion models for other grid sizes and inter-line spacing considered using smoothness constrained as well as robust inversion methods. In general, the average sensitivity and hence the resolution increases with increasing data density and decreasing interline spacing.

Discussion

The imaging abilities of different arrays are different when applied to a particular geologic structure. These differences in imaging ability are often reflected in the spatial resolution of the array, tendency to produce artefacts in the images, deviations from the true resistivity model values and the maximum depth of investigations attained by the array. Resolution is a complex function of numerous factors (e.g. electrode layout, measurement schedule, data quality, imaging algorithm, electrical conductivity distribution) and, in general, varies significantly across the image plane. The sensitivity pattern of an array is an important factor in the determination of its imaging capability. The spatial sensitivity distribution of each set of four-electrodes used for the measurements accumulates to define the spatial sensitivity of the entire survey. A simple sensitivity analysis provides some valuable insight into the resolution problem. The sensitivity analyses shows that for the combinations of orthogonal set of 2D lines, the dipole-dipole, pole-dipole and Wenner-Schlumberger arrays are more sensitive, while pole-pole, Wenner-alpha and Wenner-beta are the least sensitive arrays to 3D features. However, the more sensitive arrays have the least depth of penetration.

In theory, the inter-line spacing between the 2D lines to be combined into 3D data set shold be the same with the minimum electrode spacing. This would yield uniform electrode grids and reduced sparceness of the data set so as to obtain good quality and high resolution image. But this is not always achievable in practice. A qualitative

analysis of the inversion images and their corresponding sensitivity maps obtained from both smoothness constrained and robust inversion methods shows that inter-line spacing of less or equal to $4a$, where a is the minimum electrode separation would yield good quality and high resolution 3D images. However, inter-line spacing greater than this can still give resonable resolution but would contain more near-surface actefacts. Thus, inter-line space greater than $4a$ could be used if the near-surface feactures are not the main features of interest. The RMS error in the inversions models is relatively higher than those obtained when convention square grids are used. This is becuse the 2D lines combined to form 3D data set consist of different error characteristics. The RMS error in inversion decreases with decreasing inter-line spacing relative to the minimum electrode separation.

Conclusions

The study shows that 3D geoelectrical resistivity data set can be effectively be generated by collating parallel or orthogonal sets of 2D lines. The inter-line spacing relative to the minimum electrode separation of less or equal $4a$ will yield reliable inversion models. Inter-line spacing greater than $4a$ will produce more near-surface artefacts in the inversion models but can be very useful. Dipole-dipole, pole-dipole and Wenner-Schlumberger arrays are found to be more sensitive to 3D features among the conventional arrays studied. Two different arrays may be collated such that parallel 2D lines will consist of one array type and the perpendicular 2D lines consist of another array type. This will combined the features of the arrays: sensitivity, resolution, depth of investigations and data coverage, as may be desired to yield better 3D images than that obtained using either of the two arrays collated. The generation of 3D data sets by combining orthogonal sets of 2D lines in geoelectrical resistivity imaging speeds up field procedure and considerably reduced the time and effort involved in collecting 3D data set using square or rectangular grids. This survey design should also be applicable to geophysical investigations using induced polarization (IP) and self potential (SP).

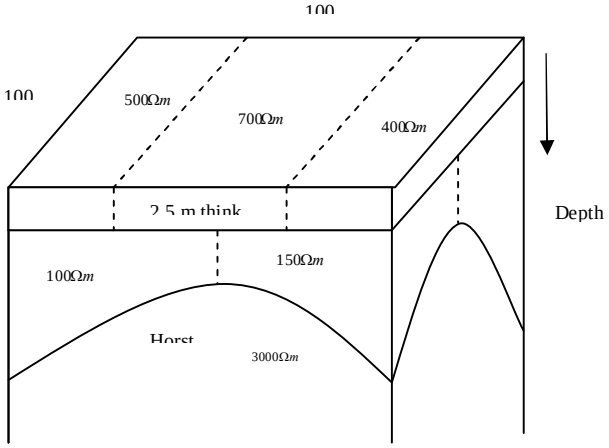

Figure 1: A three-dimensional horst model simulating a typical weathered or fractured profile developed above crystalline basement complex.

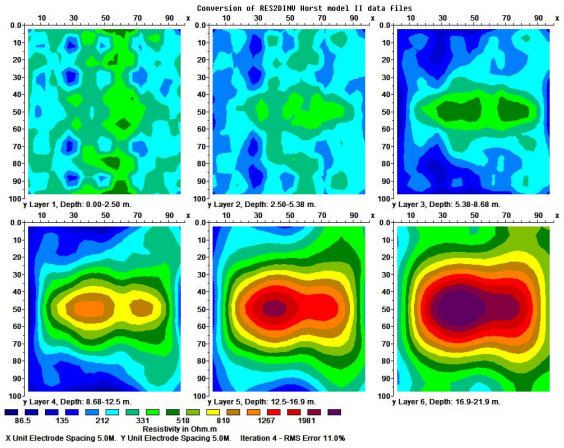

Figure 2: Horizontal depth slices of inversion model for horst model structure with grid size of 21x21 and inter-line spacing of $4a$ (Wenner-alpha array).

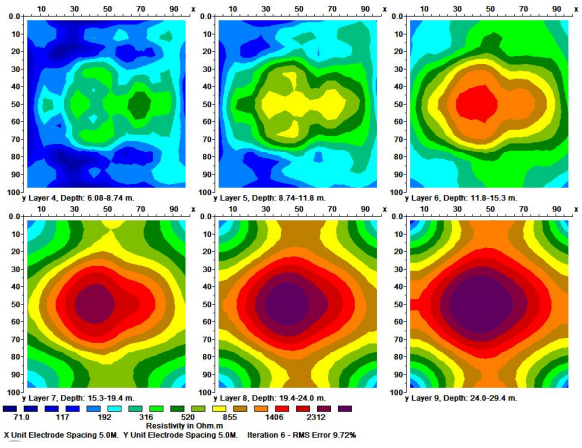

Figure 3: Horizontal depth slices of inversion model for horst model structure with grid size of 21x21 and inter-line spacing of $4a$ (Wenner-beta array).

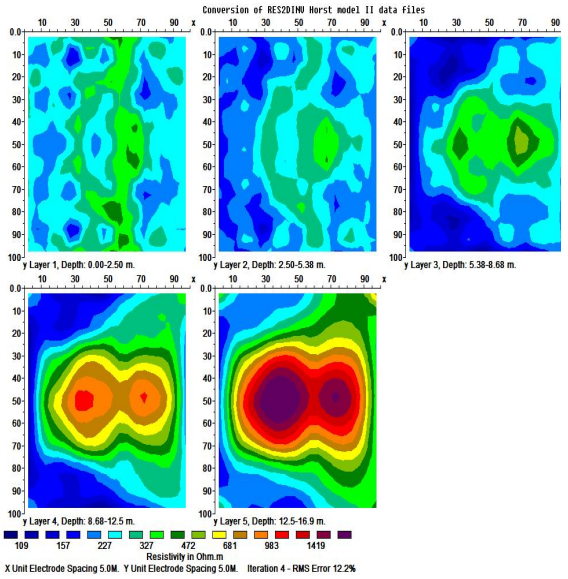

Figure 4: Horizontal depth slices of inversion model for horst model structure with grid size of 21x21 and inter-line spacing of $4a$ (Wenner-Schlumberger array).

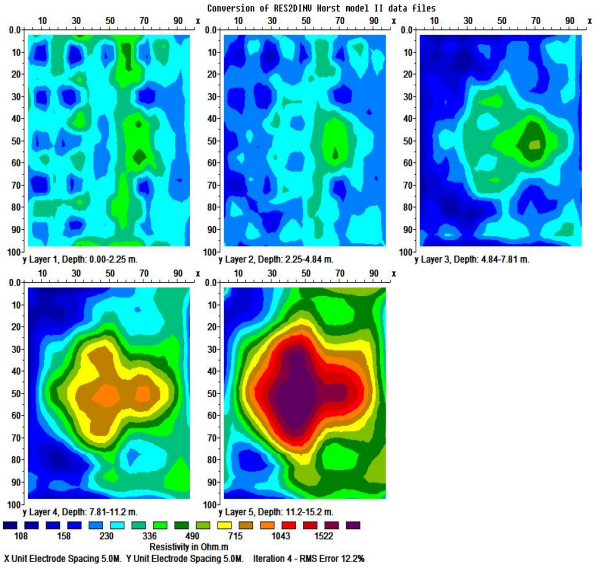

Figure 6: Horizontal depth slices of inversion model for horst model structure with grid size of 21x21 and inter-line spacing of $4a$ (pole-dipole array).

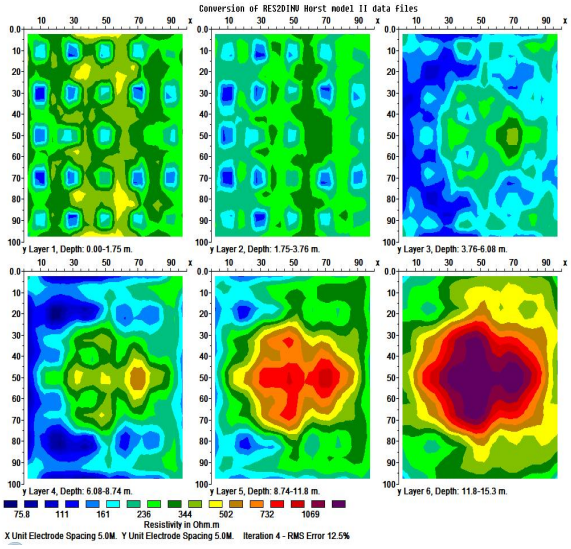

Figure 5: Horizontal depth slices of inversion model for horst model structure with grid size of 21x21 and inter-line spacing of $4a$ (dipole-dipole array).

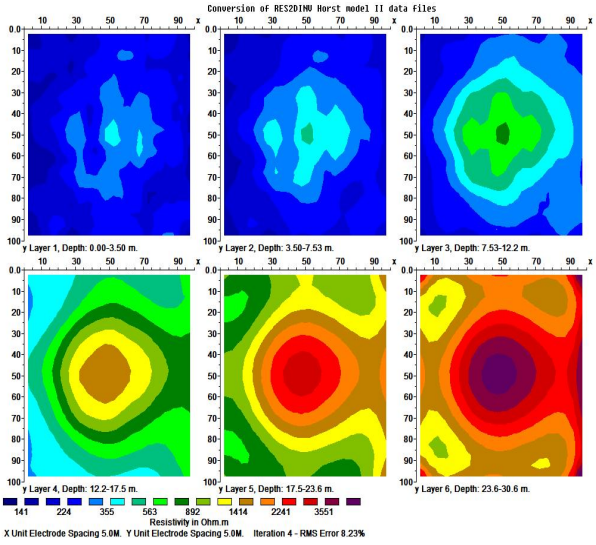

Figure 7: Horizontal depth slices of inversion model for horst model structure with grid size of 21x21 and inter-line spacing of $4a$ (pole-pole array).

Acknowledgments

The Third World Academy of Science (TWAS), Italy in collaboration with the Council of Scientific and Industrial Research (CSIR), India are gratefully acknowledge for providing the Fellowship for this study at the National Geophysical Research Institute (NGRI), Hyderabad, India.

EDITED REFERENCES

Note: This reference list is a copy-edited version of the reference list submitted by the author. Reference lists for the 2009 SEG Technical Program Expanded Abstracts have been copy edited so that references provided with the online metadata for each paper will achieve a high degree of linking to cited sources that appear on the Web.

REFERENCES

Dahlin, T., and C. Bernstone, 1997, A roll-along technique for 3D resistivity data acquisition with multi-electrode arrays: 10th Annual Meeting, Symposium on the Application of Geophysics to Engineering and Environmental Problems, Proceedings, 927–935.

deGroot-Hedlin, C., and S. C. Constable, 1990, Occam's inversion to generate smooth two-dimensional models from magnetotelluric data: Geophysics, **55**, 1613–1624.

Dey, A., and H. F. Morrison, 1979, Resistivity modeling for arbitrarily shaped three-dimensional structure: Geophsics, **44**, 753–780.

Li, Y., and D. W. Oldenburg, 1994, Inversion of 3D DC resistivity data using an approximate inverse mapping: Geophysical Journal International, **116**, 527–537.

Loke, M. H., and R. D. Barker, 1996, Rapid least-squares inversion of apparent resistivity pseudosections by a quasi-Newton method: Geophysical Prospecting, **44**, 131–152.

Park, S. K., and G. P. Van, 1991, Inversion of pole-pole data for 3D resistivity structure beneath arrays of electrodes: Geophysics, **56**, 951–960.

Press, W. H., S. A. Teukolsky, W. T. Vetterling, and B. P. Flannery, 1996, Numerical recipes in Fortran 77: The Art of Scientific Computing, 2nd ed., Cambridge Univ. Press.

Sasaki, Y., 1992, Resolution of resistivity tomography inferred from numerical simulation: Geophysical Prospecting, **40**, 453–464.

White, R. M. S., S. Collins, R. Denne, R. Hee, and P. Brown, 2001, A new survey design for 3D IP modeling at Copper Hill: Exploration Geophysics, 32, 152–155.